

† Electronic Supporting Information

Ruthenium nanoparticles ligated by cholesterol-derived NHCs and their application in the hydrogenation of arenes

Lena Rakers^{a,†}, Luis M. Martínez-Prieto^{b,†}, Angela M. López-Vinasco^b, Karine Philippot^c, Piet W. N. M. van Leeuwen^b, Bruno Chaudret^{b,*} and Frank Glorius^{a,*}

[†]These authors contributed equally to this work.

^a Organisch-Chemisches Institut, Westfälische Wilhelms Universität Münster, Corrensstraße 40, 48149 Münster, Germany, E-mail: glorius@uni-muenster.de.

^b LPCNO; Laboratoire de Physique et Chimie des Nano-Objets, UMR5215 INSA-CNRS-UPS, Institut des Sciences Appliquées, 135, Avenue de Rangueil, F-31077 Toulouse, France. E-mail: chaudret@insa-toulouse.fr.

^c LCC-CNRS; Université de Toulouse, CNRS; 205, Route de Narbonne, F31077 Toulouse, France.

Table of Content

S1. General considerations and starting materials	II
S2. Synthesis of the cholesterol-derived imidazolium salts	III
S3. Synthesis of ruthenium nanoparticles	IV
S4. HRTEM data	V
S5. WAXS data	VI
S6. Theoretical composition of Ru@chol-NHC	VI
S7. NMR data (solid, liquid and DOSY NMR)	VII
S8. IR data	XII
S9. In situ deprotonation of the imidazolium salts	XII
S10. Hydrogenation reactions	XIV
S11. Scalability test	XIV
S12. Multiple-addition tests	XV
S13. TEM data after catalysis	XV
S14. References	XVI

S1. General considerations and starting materials

All chemical operations were carried out using standard Schlenk tubes, Fischer–Porter bottle techniques or in a glove-box under argon atmosphere. Solvents were purified before use; THF, hexane and toluene (Sigma-Aldrich) by distillation under argon atmosphere and pentane (SDS) through filtration in the column of a purification apparatus (MBraun). Anhydrous trifluorotoluene was purchased from Sigma Aldrich and stored over molecular sieves under argon.

Ru(COD)(COT) was purchased from Nanomeps Toulouse, CO from Air liquide, CO (^{13}C , 99.14%) from Eurisotop, styrene (+99%) from Acros Organics. All reagents were used without purification.

Atomic absorption spectroscopy (AAS). AAS analyses of Ru@1 and Ru@2 were performed by Kolbe (Mülheim, Germany), using a Perkin Elmer AAnalyst 200 Atomic Absorption Spectrometer. The samples were prepared with a pressure digestion in a closed flask.

Wide-angle X-ray scattering (WAXS). WAXS was performed at CEMES-CNRS. Samples were sealed in 1.5 mm diameter Lindemann glass capillaries. The samples were irradiated with graphite monochromatized molybdenum $K\alpha$ (0.071069 nm) radiation and the X-ray intensity scattered measurements were performed using a dedicated two-axis diffractometer. Radial distribution functions (RDF) were obtained after Fourier transformation of the reduced intensity functions.

NMR spectroscopy. MAS-NMR analyses with and without ^1H - ^{13}C cross-polarization (CP) were performed at the LCC on a Bruker Avance 400WB instrument equipped with a 2.5 mm probe with the sample rotation frequency of 12 kHz. Measurements were carried out in a 2.5 mm ZrO_2 rotor. ^1H liquid state NMR experiments were recorded on a Bruker Avance 500 spectrometer equipped with a 5 mm triple resonance inverse Z-gradient probe. Samples were prepared in [d8] THF. ^1H signals were assigned on the basis of chemical shifts, spin–spin coupling constants, splitting patterns and signal intensities. Diffusion measurements were made using the stimulated echo pulse sequence with bipolar gradient pulses. The diffusion dimension was processed with the Laplace inversion routine CONTIN (Topspin software).

Transmission Electron Microscopy (TEM) and High resolution TEM (HRTEM). Ru-NPs were observed by TEM and HRTEM after deposition of a drop of a solution of the isolated nanoparticles after dispersion in THF on a copper grid, respectively. TEM analyses were performed at the UMS-Castaing by using a JEOL JEM 1011 CX-T electron microscope operating at 100 kV with a point resolution of 4.5 Å. The approximation of the particles mean size was made through a manual analysis of enlarged micrographs by measuring a number of particles on a given grid. HRTEM observations were carried out with a JEOL JEM 2010 electron microscope working at 200 kV with a resolution point of 2.35 Å. FFT treatments have been carried out with Digital Micrograph Version 3.7.4.

Infrared spectroscopy (IR). ATR IR-FT spectra were recorded on a Thermo Scientific Nicolet 6700 spectrometer in the range 4000–600 cm^{-1} .

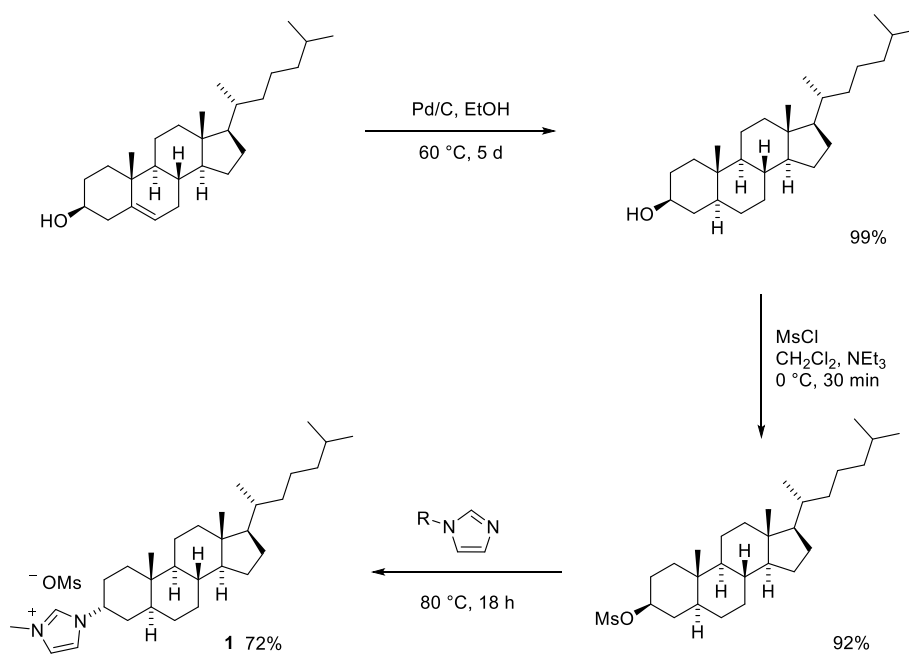
All hydrogenation reactions were carried out in Berghof High Pressure Reactors using dihydrogen gas.

Commercially available chemicals were obtained from Acros Organics, Aldrich Chemical Co., Strem Chemicals, Alfa Aesar, ABCR and TCI Europe and used as received unless otherwise stated.

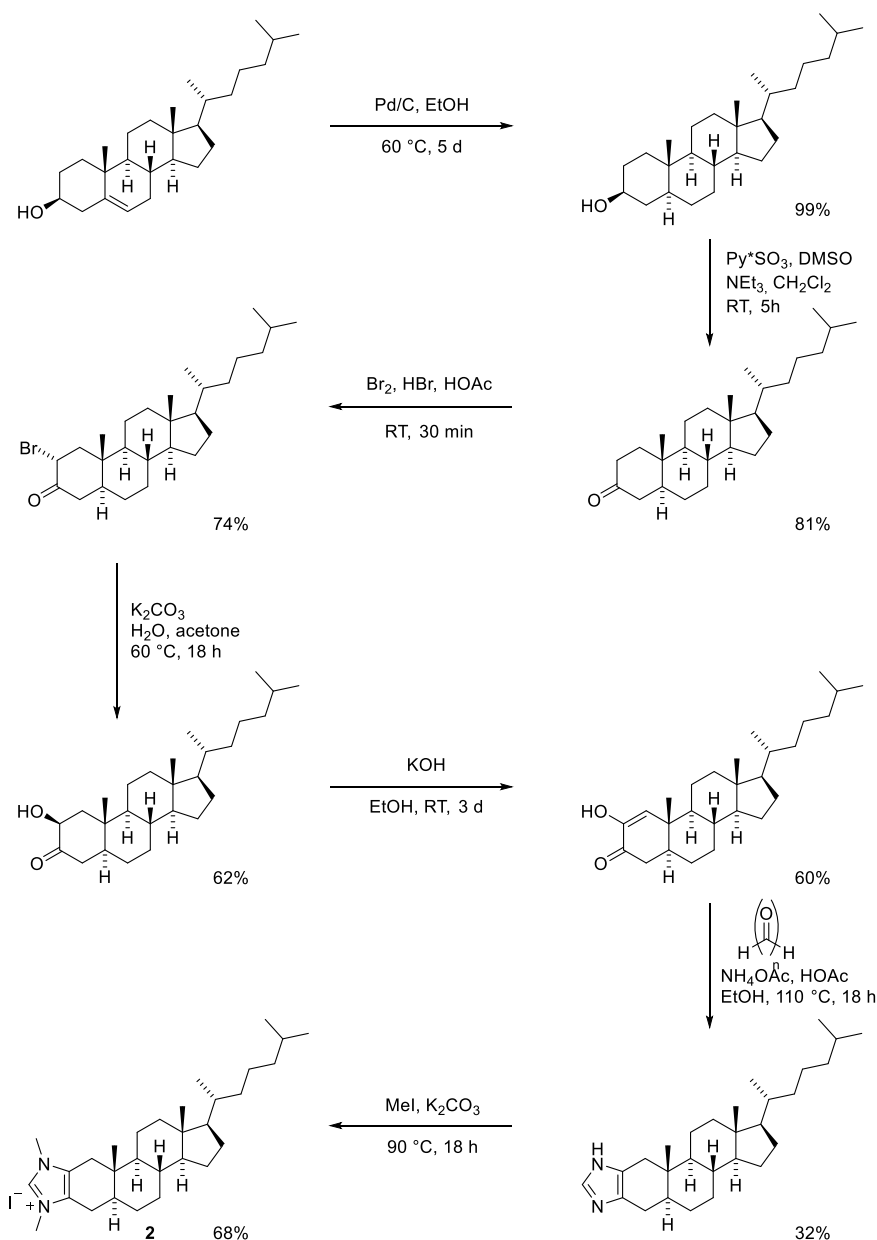
GC/MS Spectra were recorded with an Agilent Technologies 7890A GC-system with Agilent 5975C VL MSD or 5975 inert Mass Selective Detector and a HP-5MS column (0.25 mm 30 m, Film: 0.25 mm). The methods used start with the injection temperature T0. After holding this temperature for 3 min, the column is heated to temperature T1 (ramp) and this temperature is held for an additional time t (method 50_40: T0 = 50 °C, T1 = 290 °C, ramp = 40 °C/min, t = 10 min).

S2. Synthesis of the cholesterol-derived imidazolium salts

1 · HOMs and 2 · HI were synthesized according to the literature.¹



Scheme S1: Synthesis plan for imidazolium salt 1 · HOMs.



Scheme S2: Synthesis plan for imidazolium salt **2** · HI.

S3. Synthesis of ruthenium nanoparticles

Ru@1: A Schlenk flask was charged with **1**·HOMs (86.7 mg, 0.16 mmol, 0.2 equiv.) and KO^tBu (20 mg, 0.176 mmol, 0.22 equiv.). The solids were suspended in THF (50 mL) and stirred at r.t. for 20 h. After that the resulting suspension was filtered through dry celite (1 cm) under argon atmosphere and added to a 250 ml Fischer–Porter bottle charged with a cooled solution (−80 °C) of Ru(COD)(COT) (250 mg, 0.79 mmol, 1 equiv.) in 50 ml of THF (previously degassed by three freeze–pump cycles). The Fischer–Porter was pressurized with 3 bar of H₂, and the solution was allowed to reach the room temperature whilst the solution was stirred vigorously. A black homogeneous solution was immediately formed. The stirring was continued for 20 h at the room temperature. After that, the remaining H₂ pressure was released and the solution was evaporated until dryness. The black residue solid was re-dispersed in the minimum quantity of THF (~ 1 ml) and 50 ml of methanol was added. The resulting black precipitate was dried overnight under vacuum. The size of the NPs was measured by TEM on a sample of at least 100 nanoparticles, which afforded a mean value of 1.5 (0.3) nm. ICP gave the following Ru content: 51.1% Ru.

Ru@2: A Schlenk flask was charged with **2**·HI (89.5 mg, 0.16 mmol, 0.2 equiv.) and KO^tBu (20 mg, 0.176 mmol, 0.22 equiv.). The solids were suspended in THF (50 mL) and stirred at r.t. for 20 h. After that the resulting

suspension was filtered through dry celite (1 cm) under argon atmosphere and added to a 250 ml Fischer–Porter bottle charged with a cooled solution (-80 C) of Ru(COD)(COT) (250 mg, 0.79 mmol, 1 equiv.) in 50 ml of THF (previously degassed by three freeze-pump cycles). The Fischer-Porter was pressurized with 3 bar of H₂, and the solution was allowed to reach the room temperature whilst the solution was stirred vigorously. A black homogeneous solution was immediately formed. The stirring was continued for 20 h at the room temperature. After that, the remaining H₂ pressure was released and the solution was evaporated until dryness. The black residue solid was re-dispersed in the minimum quantity of THF (~ 1 ml) and 50 ml of methanol was added. The resulting black precipitate was dried overnight under vacuum. The size of the NPs was measured by TEM on a sample of at least 100 nanoparticles, which afforded a mean value of 1.4 (0.3) nm. ICP gave the following Ru content: 47.3% Ru.

S4. HRTEM data

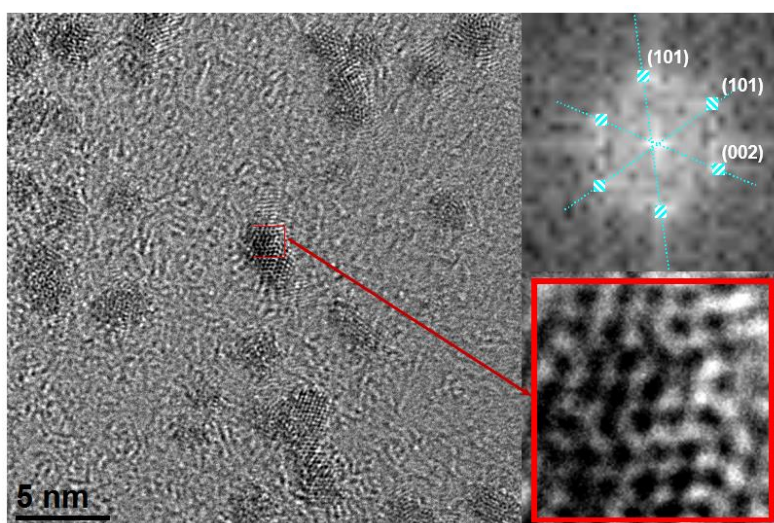


Figure S1. HRTEM image of Ru@1 (left, right bottom) and the Fourier Transform Analysis (right, top) with planar reflections. HRTEM image reveals the presence of crystalline Ru NPs retaining the hcp (hexagonal close-packed) structure. Fourier analysis applied to this image display reflections to the (101), (101) and (002) atomic planes.

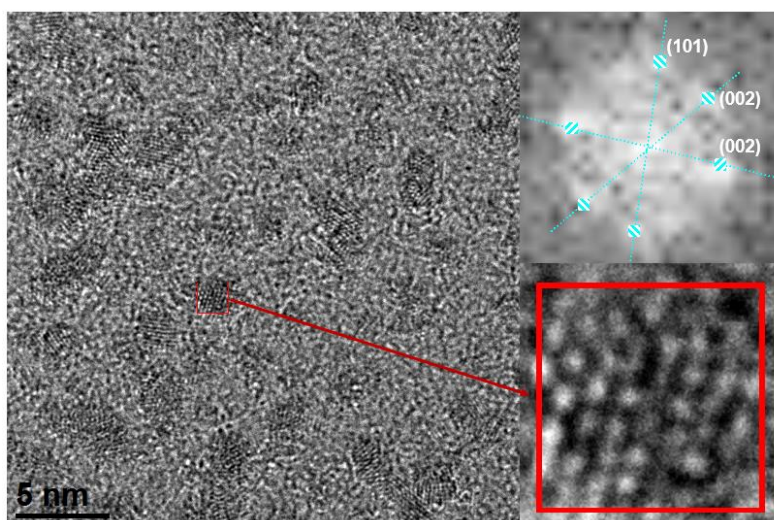


Figure S2. HRTEM image of Ru@2 (left, right bottom) and the Fourier Transform Analysis (right, top) with planar reflections. HRTEM image reveals the presence of crystalline Ru NPs retaining the hcp (hexagonal close-packed) structure. Fourier analysis applied to this image display reflections to the (101), (002) and (002) atomic planes.

S5. WAXS data

Wide-Angle X-ray Scattering (WAXS) of both NPs (Ru@1 in red and Ru@2 in green) revealed metallic NPs with a compact structure (hcp) and a coherence length of ca. 1.6 nm with no sign of oxidation.

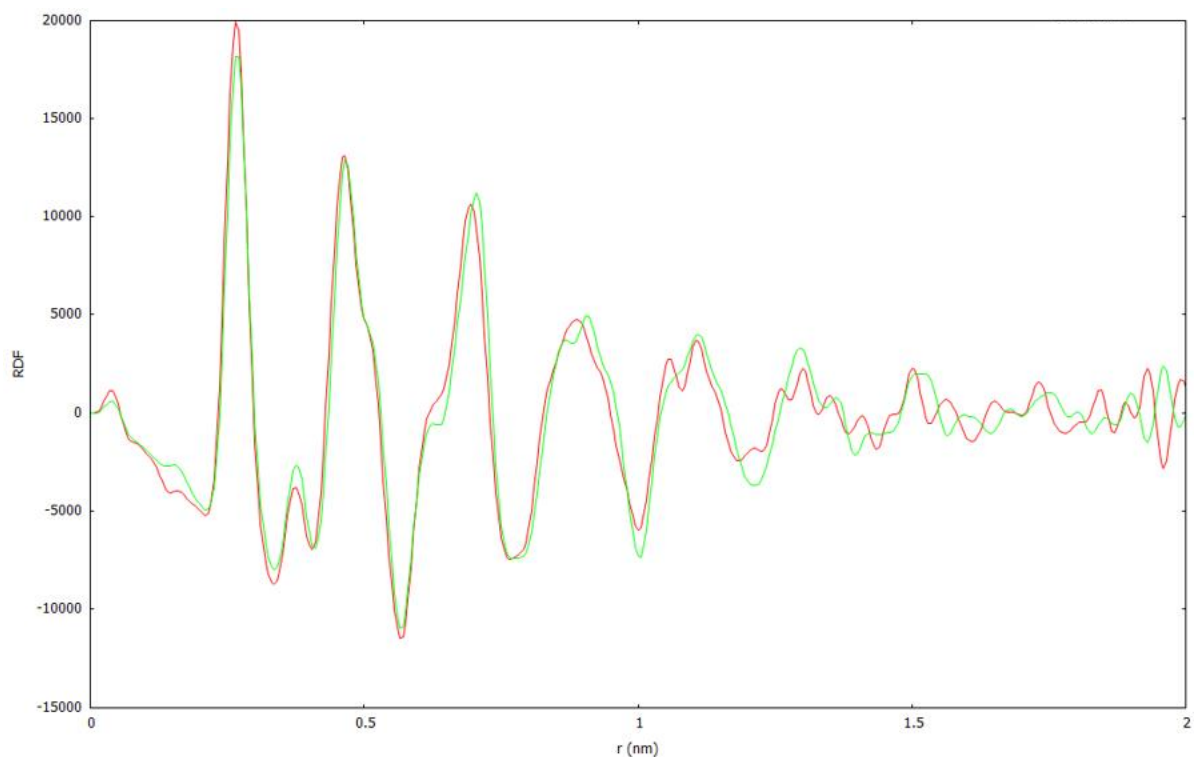


Figure S3. WAXS analysis of Ru@1 (red) and Ru@2 (green).

S6. Theoretical composition of Ru@chol-NHC

Ru NP ^a	Size (nm)	% Ru ^a	Ru:L Ratio	Ru _x /L _y ^b	Ru(s) ^c	Ru(s) _x /L _y
Ru@1	1.5 (0.3)	51.1	4.8 : 1	138/29	87	3.0
Ru@2	1.4 (0.3)	47.3	4.0 : 1	119/30	77	2.6

^a % of Ru obtained by Atomic absorption spectroscopy (AAS); ^b The approximate composition is based on the Ru/L ratio and the mean diameter measured by TEM; ^c Number of surface atoms. Approximate values obtained from the graphs of Van Hardeveld and Hartog.²

S7. NMR data (solid, liquid and DOSY NMR)

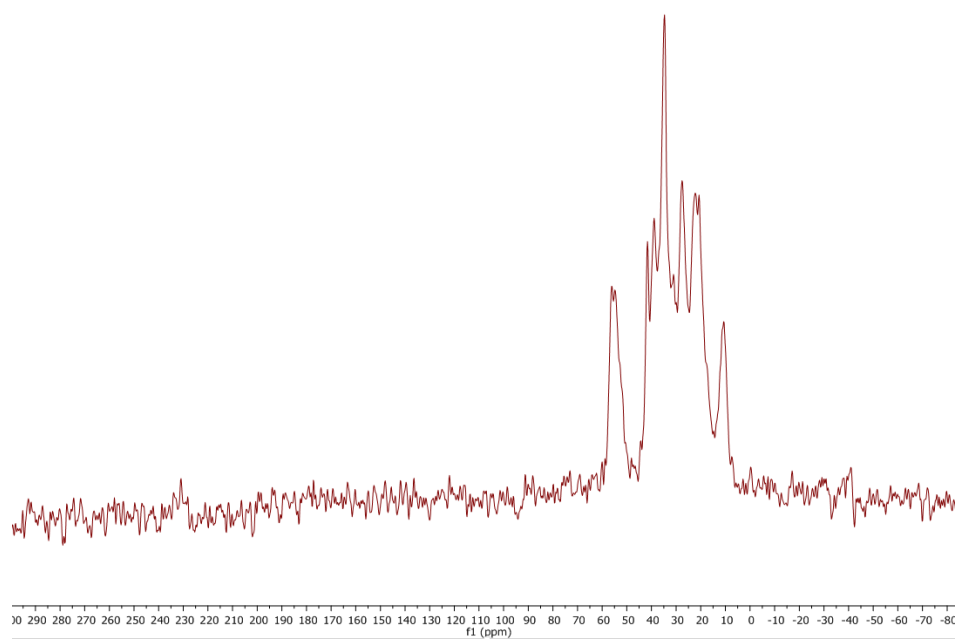


Figure S4. ^{13}C -MAS-NMR of Ru@1.

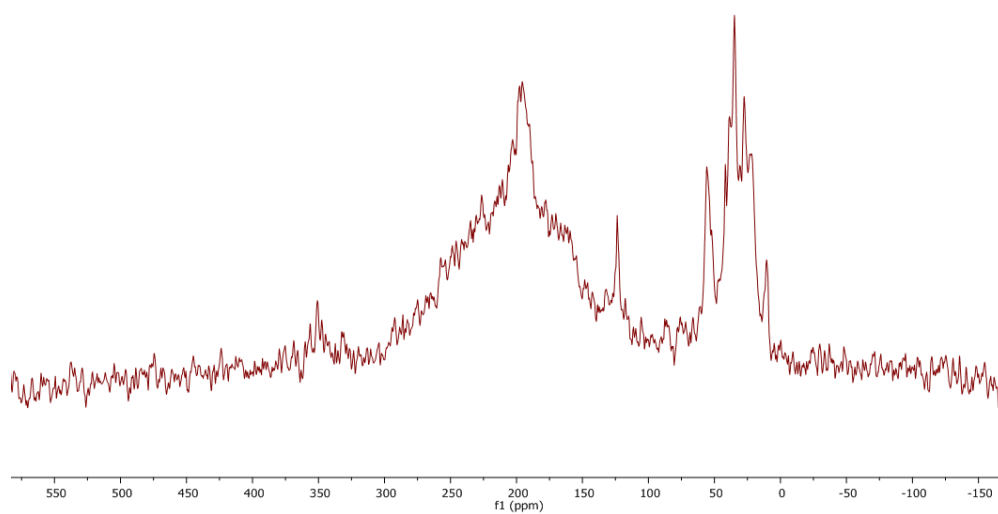


Figure S5. ^{13}C -MAS-NMR of Ru@1 after exposure to ^{13}CO (1 bar, r.t., 20 h).

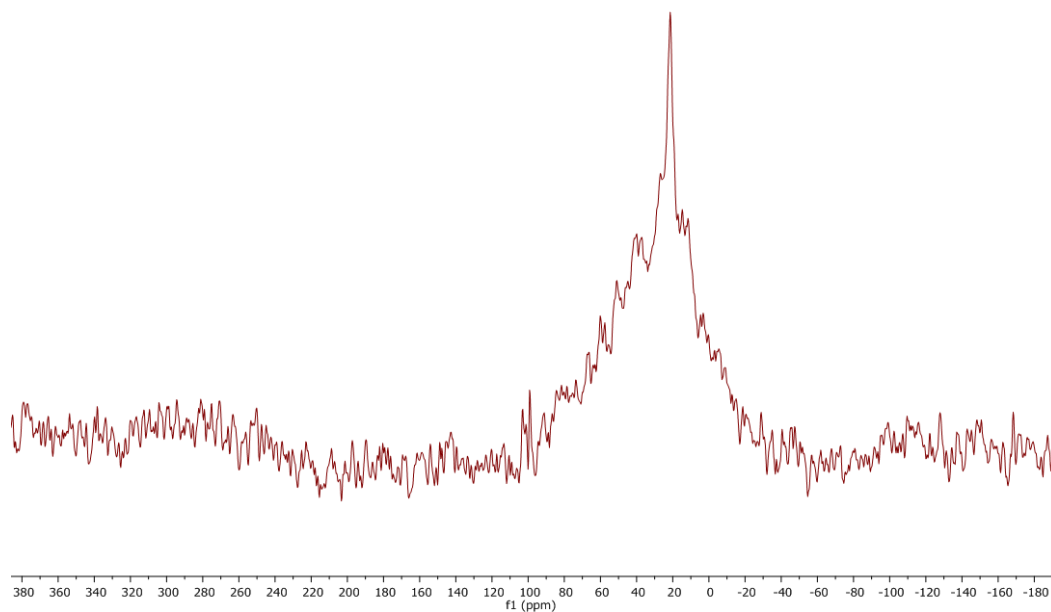


Figure S6. ^{13}C -MAS-NMR of Ru@2.

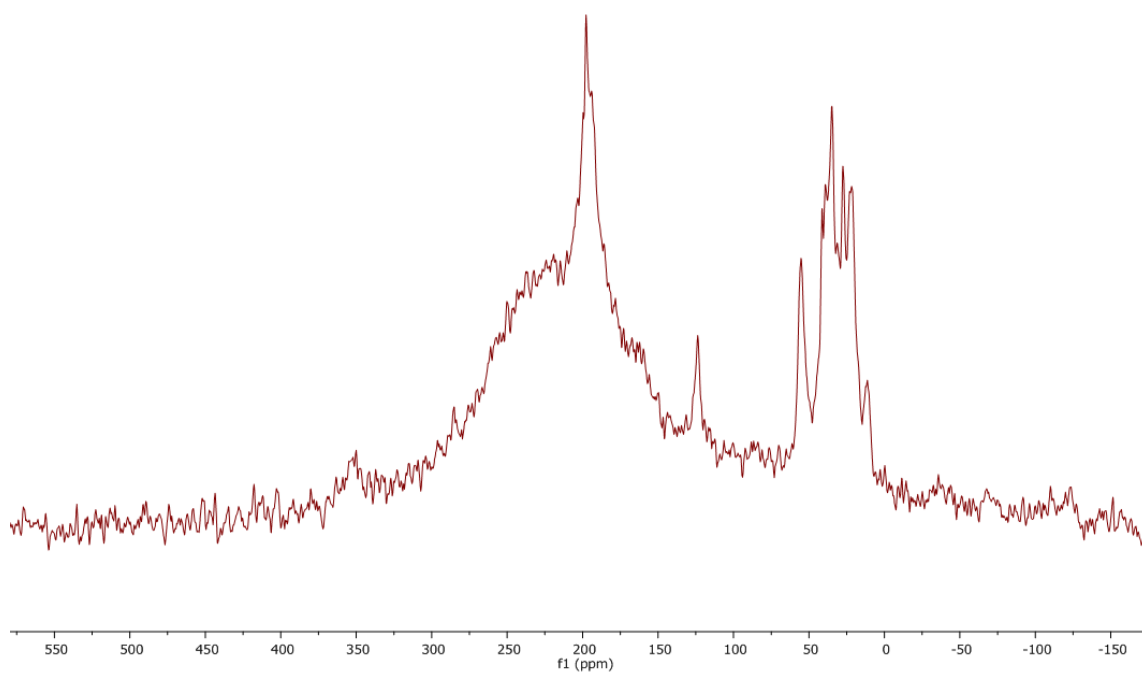


Figure S7. ^{13}C -MAS-NMR of Ru@2 after exposure to ^{13}CO (1 bar, r.t., 20 h).

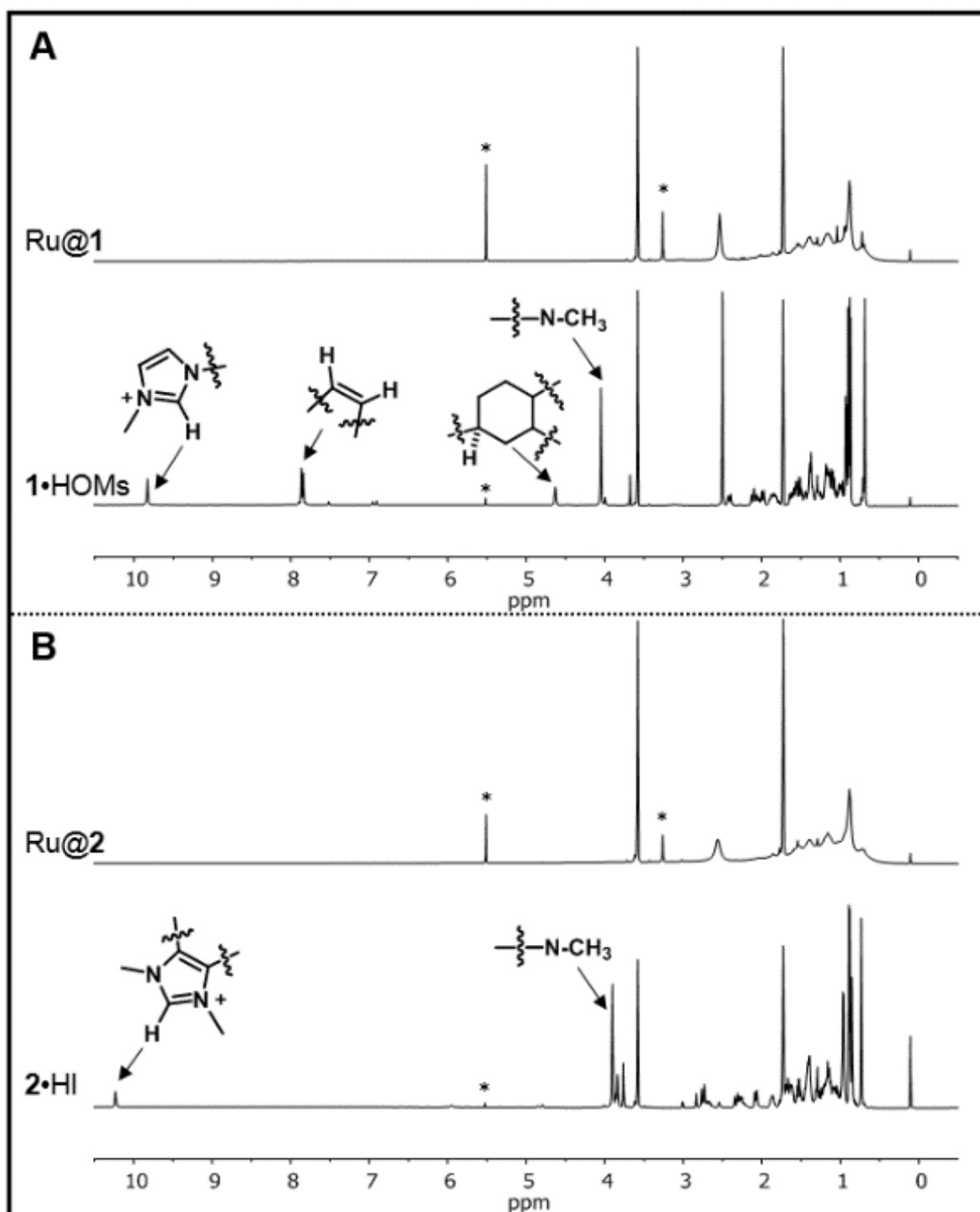


Figure S8. ¹H liquid-NMR spectra (in d₈-THF) of Ru@1 and 1·HOMs (A) and Ru@2 and 2·HI (B). Peaks that correspond to protons at or close to the imidazolium core are labelled. Peaks marked with an asterisk (*) correspond to CH₂Cl₂ (δ 5.5 ppm), which comes from the purification step of the ligands, and MeOH (δ 3.2 ppm), which arises from the purification of Ru@1 and Ru@2.

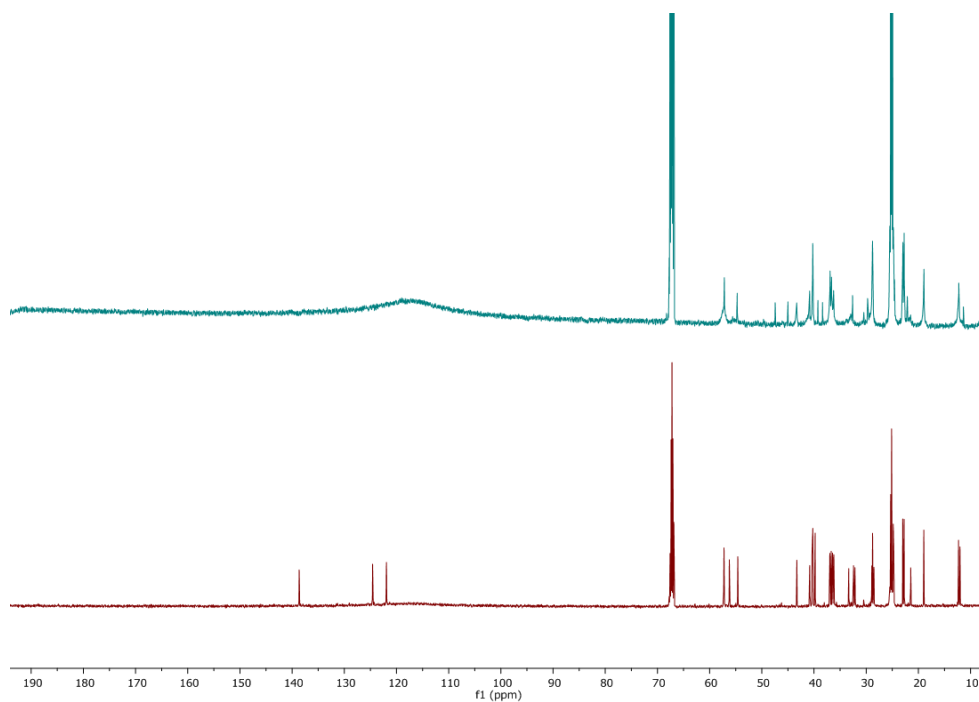


Figure S9. ^{13}C liquid-NMR spectra (in d_8 -THF) of Ru@1 (top) and 1 · HOMs (bottom).

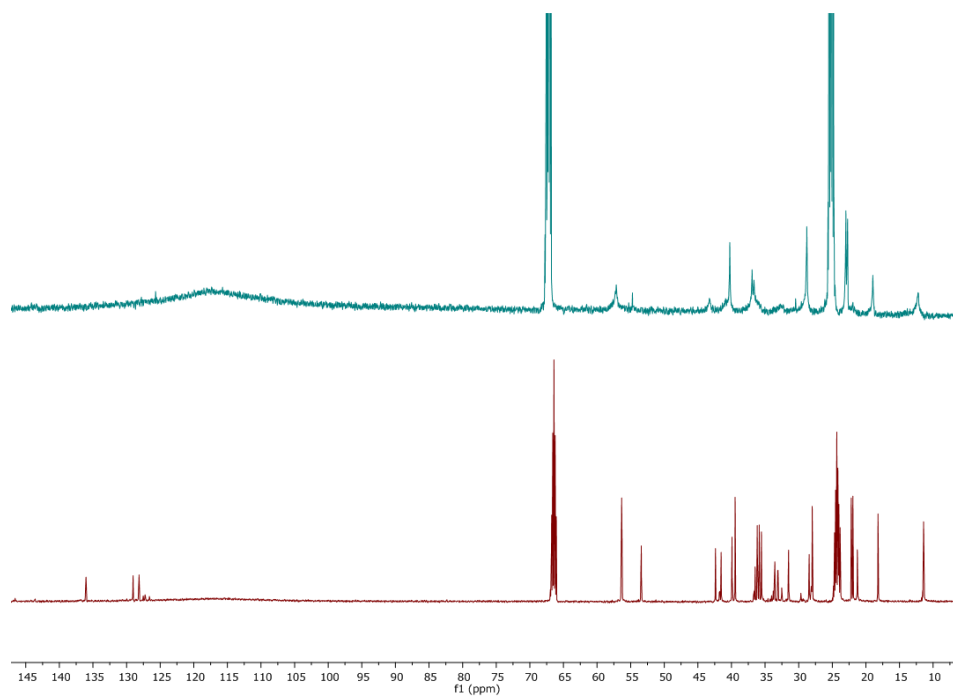


Figure S10. ^{13}C liquid-NMR spectra (in d_8 -THF) of Ru@2 (top) and 2 · HI (bottom).

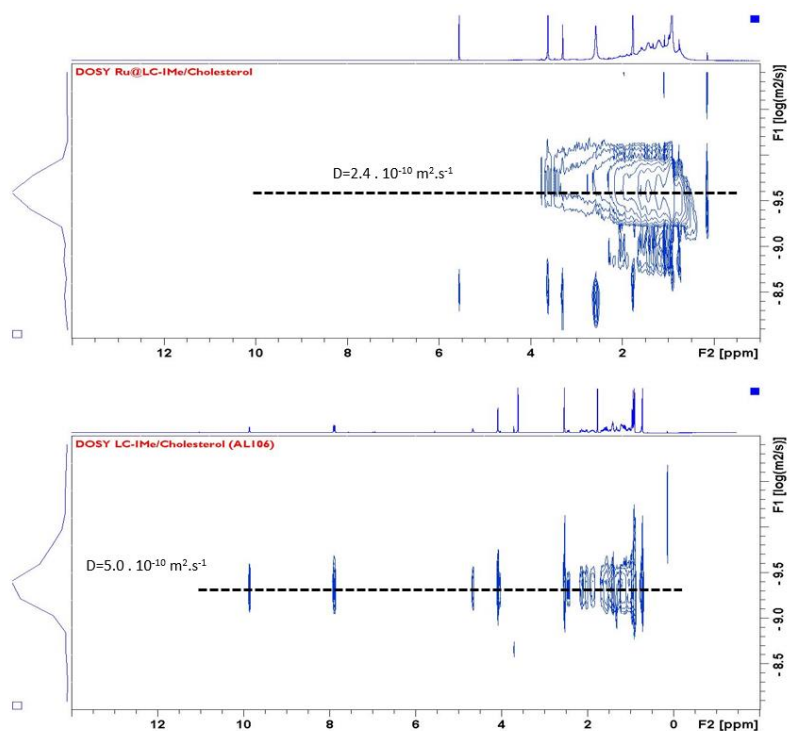


Figure S11: DOSY NMR spectra (in d_8 THF) of Ru@1 (top) and 1 · HOMs (bottom).

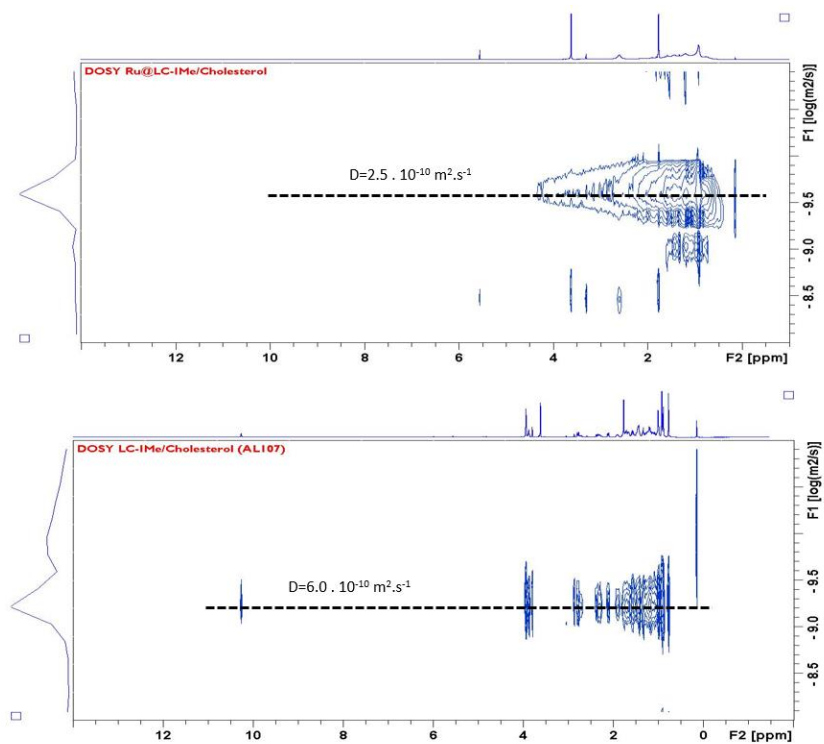


Figure S12: DOSY NMR spectra (in d_8 THF) of Ru@2 (top) and 2 · HI (bottom).

S8. IR data

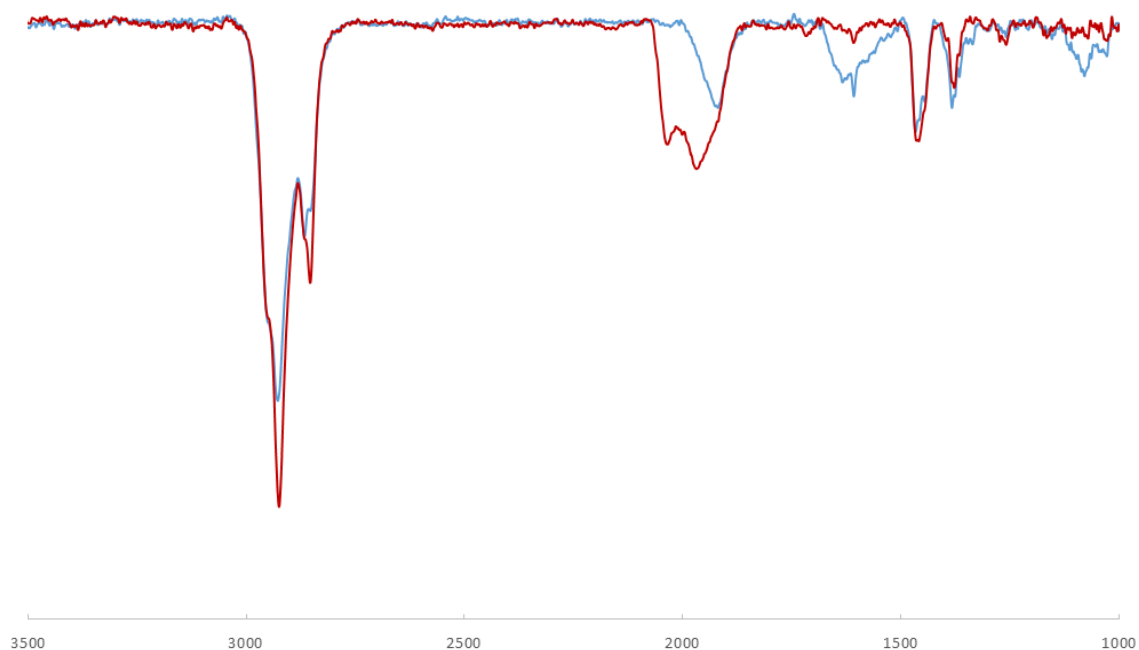


Figure S13: IR spectra recorded for Ru@1 before (blue) and after (red) exposure to CO (bubbling CO into a THF solution during 5 min).

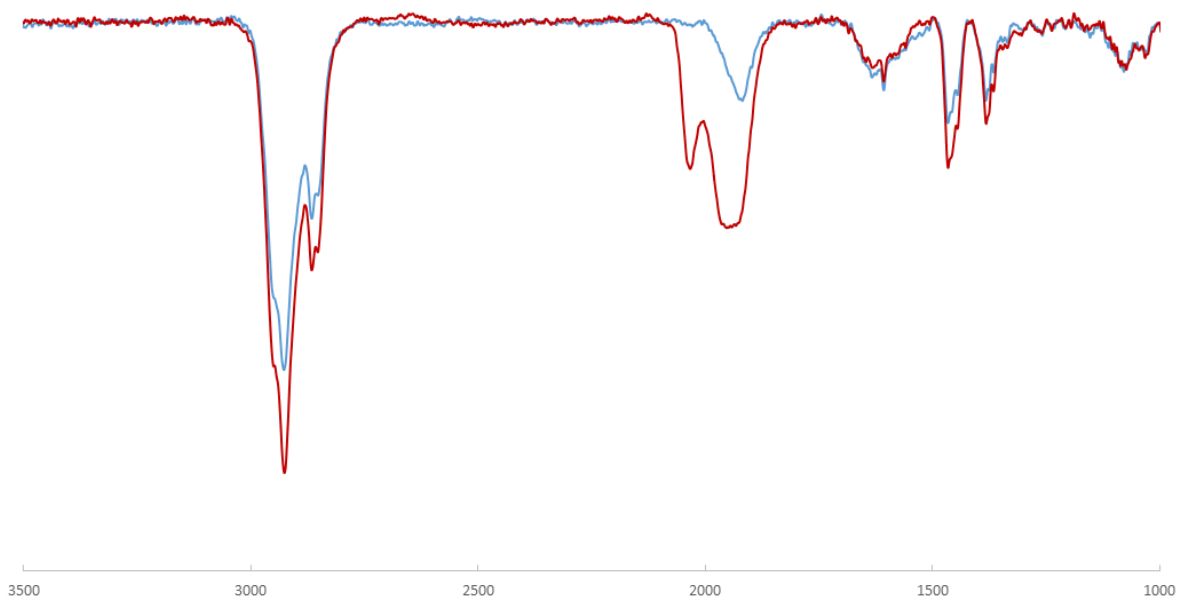


Figure S14: IR spectra recorded for Ru@2 before (blue) and after (red) exposure to CO (bubbling CO into a THF solution during 5 min).

S9. In situ deprotonation of the imidazolium salts

A flame-dried Schlenk-tube was equipped with the imidazolium salt (0.053 mmol), KO^tBu (1.1 equiv.) and d₈-THF (1 mL) and stirred at room temperature for 1 h. The resulting solution was transferred to a young-teflon NMR-tube in the glovebox and directly analyzed via NMR-spectroscopy.

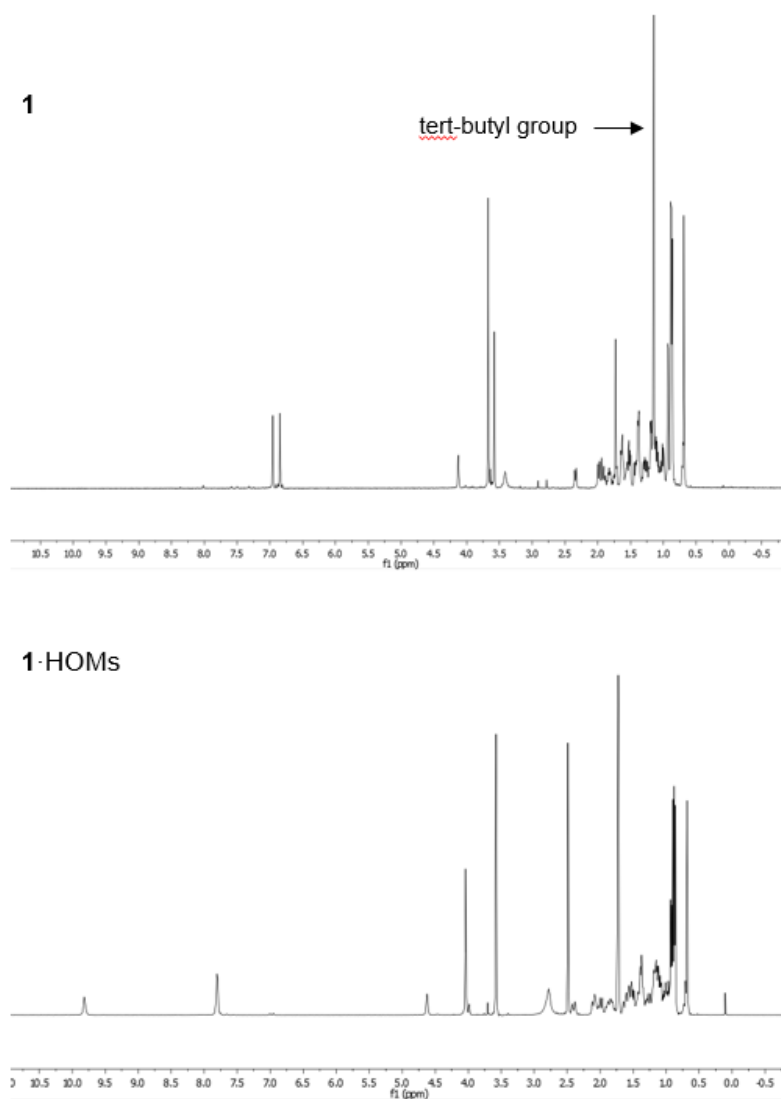


Figure S15: Comparison of the NMR of **1** (top) and **1•HOMs** (bottom). The tert-butyl signal of the in situ formed alcohol is labeled.

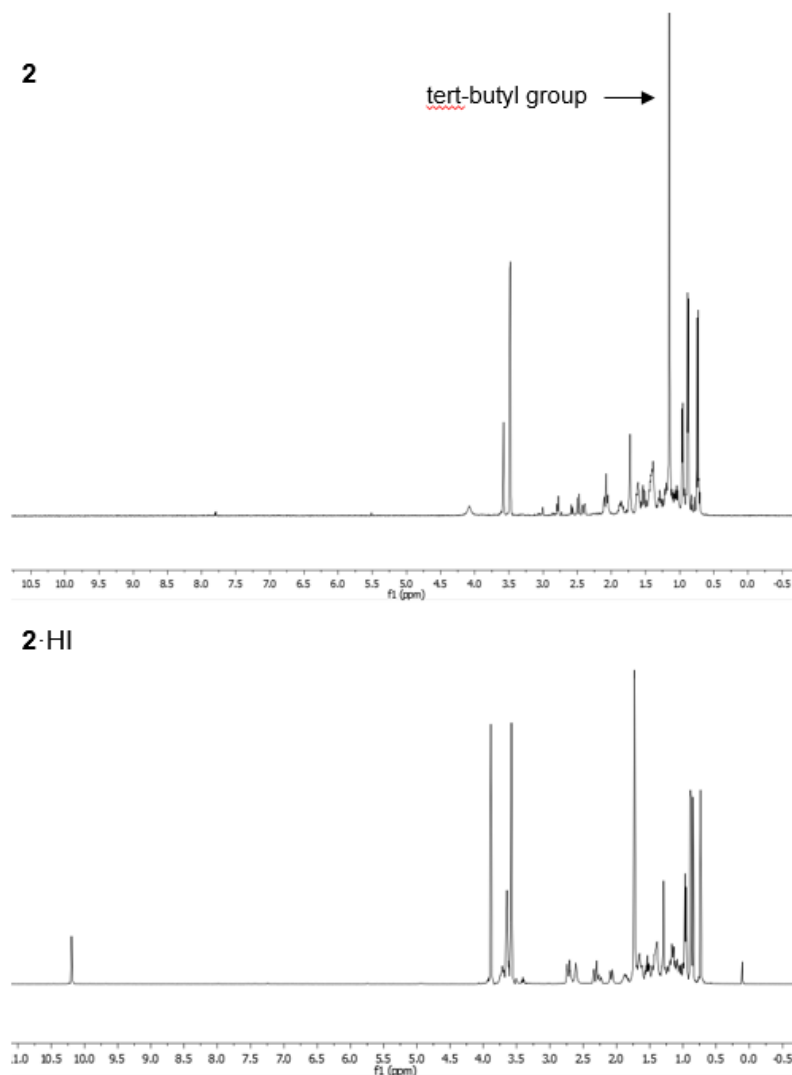


Figure S16: Comparison of the NMR of **2** (top) and **2•HI** (bottom). The tert-butyl signal of the in situ formed alcohol is labeled.

S10. Hydrogenation reactions

A screw capped glass vial was equipped with a magnetic stirring bar and was filled with Ru-NPs (2 mg). The corresponding substrate (0.2 mmol) and anhydrous THF were added (1 mL) under argon before the vial was placed in a stainless steel autoclave. The atmosphere was exchanged by carefully pressurizing/depressurizing the autoclave with hydrogen for three times. Then the indicated pressure was adjusted and the reaction mixture stirred at r.t. for 20 h. Mesitylene was added after the reaction time as internal reference (28 μ L, 1 equiv.) Reaction mixtures were analyzed by GC-MS to identify the compounds. Conversions and product ratios were determined by GC-FID.

S11. Scalability test

The scalability test was performed in the same manner as the standard hydrogenation reactions, but 2 mmol of styrene and 10 mL of THF were used.

S12. Multiple-addition tests

The multiple addition tests were done according to the standard hydrogenation reactions. After each reaction cycle (20 h), hydrogen pressure was released, styrene was added under argon (0.2 mmol) and the atmosphere was exchanged to hydrogen again. In total 0.8 mmol of styrene were added in four successive runs. After each reaction cycle, the reaction mixture was analyzed via GC-MS to identify the conversion and product formation. For both NPs a full conversion of styrene occurred for all four additions. After the first addition only ethylcyclohexane is formed in both cases. Ru@1 keeps this kind of activity for all four cycles, whereas Ru@2 shows only the hydrogenation to ethylbenzene from the second cycle on.

S13. TEM data after catalysis

After the hydrogenation of styrene the resulting reaction mixture was analyzed by TEM according to the above mentioned procedure, indicating no significant difference in NPs size.

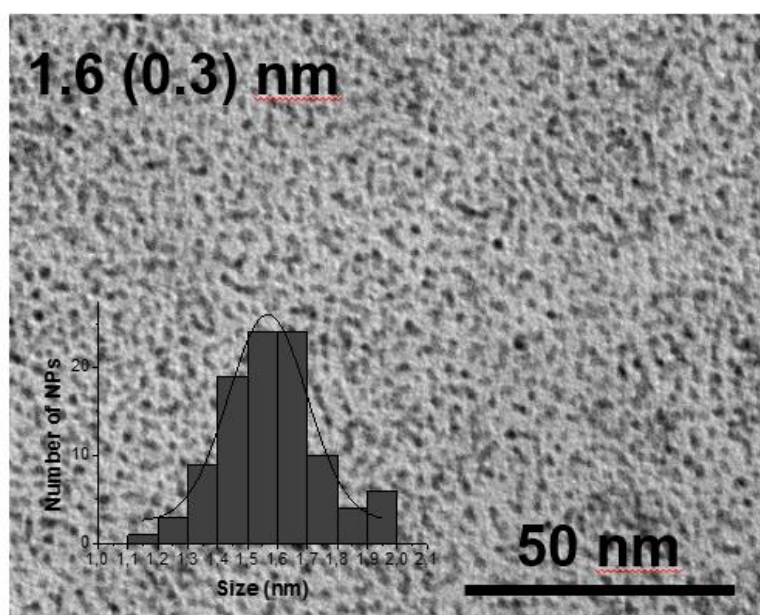


Figure S17: TEM images of Ru@1 after the hydrogenation of styrene (standard conditions).

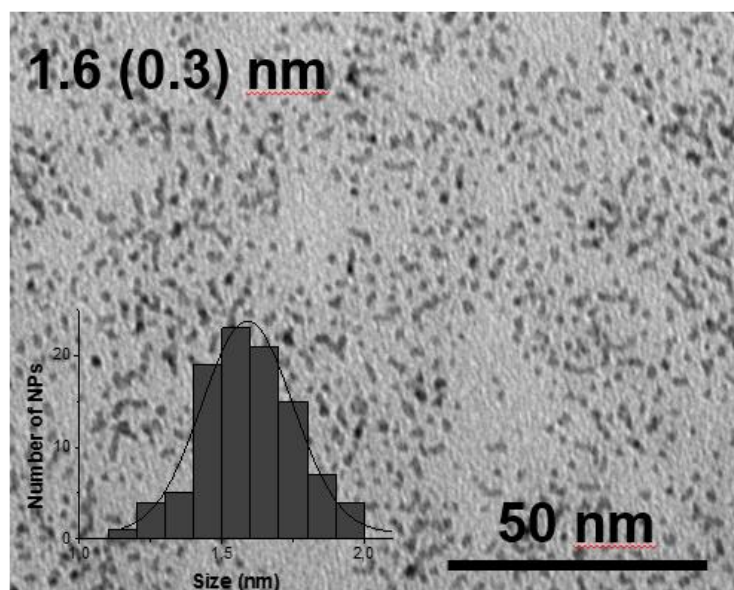


Figure S18: TEM images of Ru@2 after the hydrogenation of styrene (standard conditions).

S14. References

1. L. Rakers, D. Grill, A. L. L. Matos, S. Wulff, D. Wang, J. Börgel, M. Körsen, H. F. Arlinghaus, H.-J. Galla, V. Gerke and F. Glorius, *Cell Chemical Biology*, **2018**, doi: 10.1016/j.chembiol.2018.04.015.
2. R. van Hardeveld and F. Hartog, *Surf. Sci.*, **1969**, 15, 189